An Improved Extended Kalman Filter for Localization of a Mobile Node with NLOS Anchors

Siamak Yousefi
Department of Electrical and Computer Engineering, McGill University
Montreal, H3A0E9, QC, Canada
Email: siamak.yousefi@mail.mcgill.ca

Xiao-Wen Chang
School of Computer Science, McGill University,
Montreal, H3A0E9, QC, Canada
Email: chang@cs.mcgill.ca

Benoit Champagne
Department of Electrical and Computer Engineering, McGill University
Montreal, H3A0E9, QC, Canada
Email: benoit.champagne@mcgill.ca

***Abstract*—Tracking a mobile node using a wireless sensor network under non-line of sight (NLOS) conditions, has been considered in this work, which is of interest to indoor positioning applications. A hybrid of time difference of arrival (TDOA) and angle of arrival (AOA) measurements, suitable for tracking asynchronous targets, is exploited. The NLOS biases of the TDOA measurements and the position and velocity of the target are included in the state vector. To track the latter, we use a modified form of the extended Kalman filter (EKF) with bound constraints on the NLOS biases, as derived from geometrical considerations. Through simulations, we show that our technique can outperform the EKF and the memoryless constrained optimization techniques.**

***Keywords*—Extended Kalman filter; localization; non-line of sight; ultra wideband.**

I. INTRODUCTION

Ground-based wireless positioning has received great attention in indoor and dense urban areas due to the limitations of the global positioning system (GPS) [1]. The fine timing resolution of ultra-wideband (UWB) pulses makes them robust against multipath fading and thus, the methods based on time of arrival (TOA) can achieve good accuracy [2]. Localization techniques that directly exploit the TOA measurements require accurate target-anchor synchronization. However, if only anchor-anchor synchronization is maintained, the time difference of arrival (TDOA) data can be exploited for localization. Furthermore, the angle of arrival (AOA) measurement of UWB signal requires no tight synchronization among the anchors, and its accuracy improves with increasing the system bandwidth [3]. Although the AOA measurement of UWB signal is challenging in practice, some methods have been recently proposed for the joint measurement of TOA and AOA in UWB systems [4]. Indeed, exploiting a hybrid of angle and range information can reduce the number of required line of sight (LOS) nodes for localization.

One of the main challenges in network-based positioning remains the non-line of sight (NLOS) problem, which occurs due to the blockage of target-anchor view. In a NLOS scenario, the TOA of the first detectable signal at the receiver is larger than it would be for a direct line of sight (LOS) path, resulting in a positively biased range measurement. Also, the AOA measurements will be corrupted by a random perturbation distributed within $[0, 2\pi)$ [1]. The TOA-based localization in NLOS for a single time instant is summarized in [5]. More recently, the constrained optimization technique using sequential quadratic programming (SQP) in [6] has shown a good performance for position and NLOS bias estimation. In [6], the lower bound on the NLOS bias is set to zero and the upper bound proposed in [7] is employed. When the target is moving, the history of the past measurements along with the state equation can help in estimating a better location over time. In [8] and [9], the TDOA-AOA data are exploited for cellular and UWB indoor tracking, respectively. In both papers, Kalman filter (KF) preprocessing is applied on the received TOA data for NLOS mitigation, and the variances of the range measurements are estimated. In [9], further NLOS mitigation is done by scaling the covariance matrix of the measurement noise in an extended Kalman filter (EKF).

While these methods enable the tracking of a moving node under NLOS conditions, they have some disadvantages. First, the KF preprocessing cannot mitigate the effect of NLOS effectively, especially if the nodes are initially in a severe NLOS situation. Second, the online variance calculation of the range measurement of a moving target might not be done with good accuracy for NLOS links. In [10], the state vector of the EKF is augmented with the NLOS biases in addition to position and velocity, which helps in improving the positioning accuracy under NLOS conditions. Similar state equations have been used in particle filters (PF) developed for UWB indoor tracking of a target equipped with an inertial measurement unit (IMU) in [11], [12]. However, the computational cost of the PF grow exponentially with the size of the state vector [12], hence it is less suitable for practical applications.

In this paper, we propose a constrained form of the EKF for localization of an asynchronous mobile node under mixed LOS/NLOS conditions. The state vector of the proposed filter, similar to [10], is augmented with the NLOS biases. The steps of the constrained EKF follow those of the EKF, except for the estimation of the state vector at each time instant, where the 2-norm of a linearized vector function is minimized subject to bound constraints on the NLOS biases. These constraints are linear and depend on the geometry and the type of the measurements exploited. Since here, we use TDOA-AOA measurements for localization of an asynchronous node, the upper bound given in [7] can not be exploited. Therefore, we propose novel lower and upper bounds on the NLOS bias by exploiting the underlying geometry of the angle and range difference equations. Through simulations, we show that the proposed constrained EKF outperforms the ordinary EKF in [10], and the memoryless constrained optimization technique

 ISBN: 978-1-61208-284-4

in [6]. Other advantages of the proposed approach are its simplicity and low computational cost, which makes it suitable for practical applications.

The remainder of this paper is organized as follows: In Section II, the system model is described, and the formulation of the problem is given. The derivation of the bounds on the NLOS biases and the constrained EKF technique are described in Section III. In Section IV, illustration of simulation results are presented. Finally, Section V concludes the paper.

II. System Model and Problem Formulation

A. Range and Bearing Measurements in NLOS

We consider a 2-dimensional (2D) indoor plane on which a wireless sensor network (WSN) with M fixed anchors at known positions $\boldsymbol{p}_i = [X_i, Y_i]^T$ is deployed. The goal is to track a mobile target with unknown position $\boldsymbol{p}[k] = [x[k], y[k]]^T$ and velocity $\boldsymbol{v}[k] = [v_x[k], v_y[k]]^T$ at the k-th time instant. The synchronized anchors are placed near the boundary of the room in order to cover the area, as the anchor placement has a direct effect on the localization accuracy [5]. For the sake of simplicity, let the indices $i \in \{1, \ldots, N\}$ denote the anchors that are in NLOS, and $i \in \{N+1, \ldots, M\}$ denote the anchors with LOS measurements. We assume that the NLOS links can be identified accurately at every time instant. To this end, NLOS identification techniques based on hypothesis testing have been proposed in [8], [9], [13], [5]. Furthermore, NLOS identification based on the features of the received UWB timing pulse can yield a good result [14].

The range measurement for the i-th anchor, $z_i[k]$, is obtained by multiplying the corresponding TOA measurement with the speed of wave propagation. The set of range equations for the M anchors are

$$z_i[k] = d_i[k] + \epsilon[k] + b_i[k] + n_i[k], \quad i = 1, \ldots, M \quad (1)$$

where $d_i[k] = \sqrt{(x[k] - X_i)^2 + (y[k] - Y_i)^2}$ is the true range, $\epsilon[k]$ is proportional to the relative clock offset between the target and the anchors (the clock offset is common among the anchors as they are synchronized), $b_i[k]$ is the NLOS bias which is a positive random variable for $i \in \{1, \ldots, N\}$ and zero for $i \in \{N+1, \ldots, M\}$, and $n_i[k]$ is the measurement noise. The distribution of the NLOS bias is location dependent and time varying; therefore, assuming a priorly known distribution is not practical. However, as the target moves, the instantaneous value of the NLOS bias can be approximately modelled as a random walk

$$b_i[k+1] = b_i[k] + w_b[k], \quad i = 1, \ldots, N \quad (2)$$

where the increment $w_b[k]$ is a uniform random variable with zero-mean and variance $\sigma^2_{w_b}$ [11], [12]. The measurement noise in (1) is modelled as a normal random variable with zero-mean and variance $\sigma^2_{n_i}[k]$. In UWB systems, the variance of this noise can be represented as

$$\sigma^2_{n_i}[k] = \sigma_0^2 d_i^{\beta}[k], \quad (3)$$

where σ_0 is a proportionality constant and β is the path-loss exponent, which might have different values based on the environment, e.g., $\beta = 2$ for LOS and $\beta = 3$ for NLOS have been considered in [15].

The AOA can be measured jointly with the TOA by means of UWB antenna arrays as done in [4]. The AOA of the NLOS anchors are discarded as done in [9], since they are corrupted by random perturbations uniformly distributed in the interval $[0, 2\pi)$. The AOA of the LOS anchors with respect to a reference coordinate system are

$$\theta_i[k] = \tan^{-1}\Big(\frac{y[k] - Y_i}{x[k] - X_i}\Big) + n_{\theta_i}[k], \quad i = N+1, \ldots, M \quad (4)$$

where the measurement error, $n_{\theta_i}[k]$, is normally distributed with zero-mean and variance σ^2_{θ}.

The clock offset parameter $\epsilon[k]$ is cancelled out by subtracting the measured range of each anchor in (1) from a reference anchor, which amounts to employing TDOA measurements. If all the anchors are in NLOS, i.e., $N = M$, then the range difference achieved through subtraction has either a positive or negative bias. For this scenario, the techniques in [8] and [9] can be employed, where KF preprocessing is used for smoothing and variance calculation. However, as mentioned earlier, KF smoothing can not mitigate the effect of the NLOS bias efficiently. In this paper, to overcome this limitation, we assume instead that there is at least one LOS range measurement available, i.e., $N < M$. In this case, the range difference measurements can be obtained with respect to a selected reference LOS anchor, which for simplicity is indexed by M. If multiple LOS anchors are available, then amongst them, we propose to select as reference anchor the one which is closest to the target, i.e., with respect to which all the LOS range differences are positive. Since a smaller measured range is usually less likely to be in NLOS compared to a larger range, this selection of the reference anchor is relatively robust against false alarm in NLOS detection. Furthermore, the choice of the reference anchor can change over time due to the transition from LOS to NLOS. If the i-th anchor changes from NLOS to LOS, then $b_i[k]$ becomes zero, while if the i-th anchor changes from LOS to NLOS then the bias changes from zero to a positive random value. Therefore, if the reference anchor goes through such a transition, then another anchor which is in LOS has to be selected as the reference. If there are two or more LOS anchors, then by rejecting the NLOS range measurements, the location can be estimated without ambiguity, however, the performance highly depends on the AOA measurement error, which might have a large error in some applications.

The range difference equations hence take the form

$$\Delta z_i[k] = \begin{cases} \Delta d_i[k] + b_i[k] + \Delta n_i[k] & i = 1, \ldots, N \\ \Delta d_i[k] + \Delta n_i[k] & i = N+1, \ldots, M-1 \end{cases}$$

where $\Delta z_i[k] = z_i[k] - z_M[k]$, $\Delta d_i[k] = d_i[k] - d_M[k]$ and $\Delta n_i[k] = n_i[k] - n_M[k]$.

B. Problem Formulation

Let the unknown state vector, which includes the biases, be defined as $\boldsymbol{s}[k] = [x[k], y[k], v_x[k], v_y[k], b_1[k], \ldots, b_N[k]]^T$. The measurement equation can be expressed as

$$\boldsymbol{y}[k] = \boldsymbol{h}(\boldsymbol{s}[k]) + \boldsymbol{n}[k], \quad (5)$$

 ISBN: 978-1-61208-284-4

where

$$\boldsymbol{y}[k] = \begin{bmatrix} \Delta z_1[k] \\ \vdots \\ \Delta z_N[k] \\ \Delta z_{N+1}[k] \\ \vdots \\ \Delta z_{M-1}[k] \\ \theta_{N+1}[k] \\ \vdots \\ \theta_M[k] \end{bmatrix}, \quad \boldsymbol{h}(\boldsymbol{s}[k]) = \begin{bmatrix} \Delta d_1[k] + b_1[k] \\ \vdots \\ \Delta d_N[k] + b_N[k] \\ \Delta d_{N+1}[k] \\ \vdots \\ \Delta d_{M-1}[k] \\ \tan^{-1}\left(\frac{y[k]-Y_{N+1}}{x[k]-X_{N+1}}\right) \\ \vdots \\ \tan^{-1}\left(\frac{y[k]-Y_M}{x[k]-X_M}\right) \end{bmatrix},$$

and $\boldsymbol{n}[k]$ is a normally distributed random vector with zero-mean and covariance matrix $\boldsymbol{R}[k]$. We assume uncorrelated range and angle measurements, i.e.,

$$\boldsymbol{R}[k] = \begin{bmatrix} \boldsymbol{R}_r[k] & \boldsymbol{0} \\ \boldsymbol{0} & \boldsymbol{R}_\theta[k] \end{bmatrix}, \tag{6}$$

in which we let

$$\boldsymbol{R}_r[k] = \sigma^2_{n_M}[k]\mathbf{1}_{M-1}\mathbf{1}^T_{M-1} + \mathrm{diag}(\sigma^2_{n_1}[k], \ldots, \sigma^2_{n_{M-1}}[k]),$$

$$\boldsymbol{R}_\theta[k] = \sigma^2_\theta \boldsymbol{I}_{M-N},$$

where $\mathbf{1}_{M-1} = [1, \ldots, 1]^T$ of size $m \times 1$, and $\boldsymbol{I}_m$ is the identity matrix of size $m \times m$.

The state equation is given by

$$\boldsymbol{s}[k+1] = \boldsymbol{A}_a \boldsymbol{s}[k] + \boldsymbol{B}_a \boldsymbol{w}_a[k], \tag{7}$$

where

$$\boldsymbol{A}_a = \begin{bmatrix} \boldsymbol{A} & \boldsymbol{0} \\ \boldsymbol{0} & \boldsymbol{I}_N \end{bmatrix}, \ \boldsymbol{B}_a = \begin{bmatrix} \boldsymbol{B} & \boldsymbol{0} \\ \boldsymbol{0} & \boldsymbol{I}_N \end{bmatrix}, \ \boldsymbol{w}_a[k] = \begin{bmatrix} \boldsymbol{w}[k] \\ \boldsymbol{w}_b[k] \end{bmatrix},$$

$$\boldsymbol{A} = \begin{bmatrix} 1 & 0 & \delta t & 0 \\ 0 & 1 & 0 & \delta t \\ 0 & 0 & 1 & 0 \\ 0 & 0 & 0 & 1 \end{bmatrix}, \quad \boldsymbol{B} = \begin{bmatrix} 0.5\delta t^2 & 0 \\ 0 & 0.5\delta t^2 \\ \delta t & 0 \\ 0 & \delta t \end{bmatrix},$$

$\boldsymbol{w}[k]$ is normally distributed with zero mean and covariance matrix $\mathrm{diag}(\sigma^2_x, \sigma^2_y)$, $\boldsymbol{w}_b[k]$, which is uncorrelated with $\boldsymbol{w}[k]$, has a uniform distribution with zero mean and covariance matrix $\sigma^2_{w_b}\boldsymbol{I}_N$, and δt is the time step duration.

The aim is to find the position and velocity of the target at the k-th time instant, i.e., $\boldsymbol{x}[k]$ and $\boldsymbol{v}[k]$, based on all the past and current measurements $\boldsymbol{y}[j]$ for time instants $j \in \{1, \ldots, k\}$. A common approach is to employ the EKF as done in [10]. However, in this work, we improve the estimation accuracy by taking advantage of extra information, in the form of practical constraints on the NLOS bias $b_i[k]$, which is derived in the sequel.

III. Proposed Technique

We first determine more accurate constraints on the NLOS biases through the geometry of the network and then propose the improved EKF algorithm.

A. Constraint Region

We are interested in tight lower and upper bounds on the NLOS bias $b_i[k]$ when TDOA-AOA measurements are exploited. Note that in UWB systems, the range measurement noise is small compared to the NLOS bias. Also the AOA measurement error of a LOS link is relatively low. Thus, in deriving these bounds we assume that the noise terms are negligible, i.e., $\Delta z_i[k] = \Delta d_i[k] + b_i[k]$ for $i \in \{1 \ldots, N\}$ and $\tan(\theta_M[k]) = (y[k] - Y_M)/(x[k] - X_M)$. Herein, we consider the case where only one LOS anchor is available, although the bounds are still applicable when more LOS anchors exist.

For illustrative purposes, consider the physical setting of the anchors and target shown in Fig. 1. The measured AOA at the LOS reference anchor, $\theta_M[k]$, defines a line segment passing through the target position and denoted as L_M. Furthermore, the true (unbiased) ranges, $\Delta d_i[k]$, define a set of hyperbolas, denoted as H^u_{iM} and given by

$$\|\boldsymbol{x} - \boldsymbol{p}_i\| - \|\boldsymbol{x} - \boldsymbol{p}_M\| = \Delta d_i[k], \quad i = 1, \ldots, N \tag{8}$$

Therefore, if we know $\Delta d_i[k]$, then the target position can be found by intersecting one of the hyperbolas H^u_{iM} with the AOA line segment L_M. Due to the NLOS condition, we measure $\Delta z_i[k]$, which is biased compared to $\Delta d_i[k]$. If $|\Delta z_i[k]| \leq \|\boldsymbol{p}_i - \boldsymbol{p}_M\|$, then all the points $\boldsymbol{x}$, for which the difference of the distances from the i-th and the M-th anchor is equal to $\Delta z_i[k]$ are located on a different set of hyperbolas, denoted as H^b_{iM} and given by

$$\|\boldsymbol{x} - \boldsymbol{p}_i\| - \|\boldsymbol{x} - \boldsymbol{p}_M\| = \Delta z_i[k], \quad i = 1, \ldots, N \tag{9}$$

We note, however, that, if the bias is large, we might face a situation where $\Delta z_i[k] > \|\boldsymbol{p}_i - \boldsymbol{p}_M\|$, and then there is no point on the plane satisfying (9). In this case, it is convenient to redefine $\Delta z_i[k]$ by thresholding it to its maximum permissible value, i.e., $\Delta z_i[k] \leftarrow \min(\Delta z_i[k], \|\boldsymbol{p}_i - \boldsymbol{p}_M\|)$. If $\Delta z_i[k]$ is replaced by $\|\boldsymbol{p}_i - \boldsymbol{p}_M\|$, then (9) becomes a ray passing through $\boldsymbol{p}_M$. In the sequel, $\Delta z_i[k]$ refers to the range difference measurement after being readjusted in this way.

Since the bias is always positive, a trivial lower bound on $b_i[k]$ is 0. Also, since by definition $b_i[k] = \Delta z_i[k] - \Delta d_i[k]$, an upper bound on $b_i[k]$ can be found by finding a lower bound on $\Delta d_i[k]$. Invoking the triangle inequality, it follows that $\Delta d_i[k] \geq -\|\boldsymbol{p}_i - \boldsymbol{p}_M\|$. Thus, loose lower and upper bounds on $b_i[k]$ might be set as

$$0 \leq b_i[k] \leq \Delta z_i[k] + \|\boldsymbol{p}_i - \boldsymbol{p}_M\|. \tag{10}$$

However, we can achieve tighter lower and upper bounds on $b_i[k]$ by taking advantage of the geometry.

Let the hyperbola H^b_{iM} intersects with the line segment L_M at $\boldsymbol{q}_i[k]$, and define $r_i[k] = \|\boldsymbol{q}_i[k] - \boldsymbol{p}_M\|$. By expressing the equation of hyperbola (9) in polar coordinates, it follows that

$$r_i[k] = \frac{\|\boldsymbol{p}_i - \boldsymbol{p}_M\|^2 - \Delta z_i^2[k]}{2\big(\Delta z_i[k] + \|\boldsymbol{p}_i - \boldsymbol{p}_M\| \cos(\theta_M[k] - \varphi_i)\big)}, \tag{11}$$

where φ_i is the angle between the horizontal axis and the line segment connecting the *i*-th and the reference anchors. If the bias does not exist in the range difference equation, then $r_i[k]$ is equal to $d_M[k]$. However, since $\Delta z_i[k] \geq \Delta d_i[k]$, $r_i[k]$ is biased compared to $d_M[k]$. It can be verified analytically that

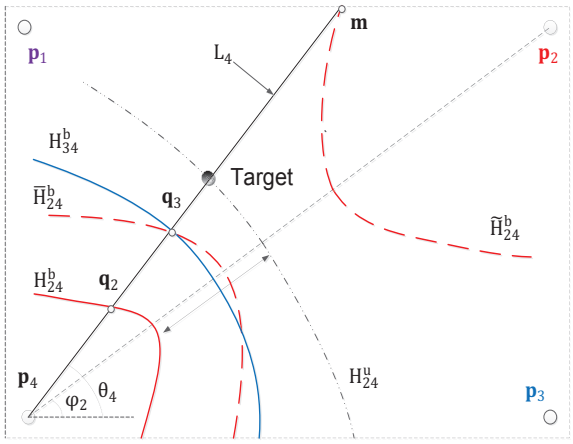

Fig. 1. Geometry of the nodes in 2-D. The anchor with index $M = 4$ is the reference LOS anchor and the other anchors are in NLOS. The time index k is omitted for convenience.

$r_i[k]$ in (11) is a monotonically decreasing function of $\Delta z_i[k]$ with upper bound

$$r_i[k] \leq d_M[k], \qquad i = 1, \ldots, N \tag{12}$$

Let us define $r_j[k] = \max\{r_i[k], i = 1, \ldots, N\}$; then $r_j[k] \leq d_M[k]$, i.e., the distance of the target from the reference anchor has to be at least $r_j[k]$. Note that in case $\Delta z_i[k]$ is replaced by $\|\boldsymbol{p}_i - \boldsymbol{p}_M\|$, $r_i[k] = 0$ and (12) is satisfied. For the vector $\boldsymbol{q}_j[k]$, define in turn

$$\Delta \bar{z}_i[k] = \|\boldsymbol{q}_j[k] - \boldsymbol{p}_i\| - \|\boldsymbol{q}_j[k] - \boldsymbol{p}_M\|, \tag{13}$$

which means that $\boldsymbol{q}_j[k]$ is located on another set of hyperbolas, denoted as $\bar{H}^b_{iM}$, representing the points for which the distance difference from the i-th and M-th anchors is $\Delta \bar{z}_i[k]$. For example, in Fig. 1, $\bar{H}^b_{24}$ passes through $\boldsymbol{q}_3$ where $j = 3$. Similar to (11), by intersecting $\bar{H}^b_{iM}$ and the line segment L_M, we have that

$$r_j[k] = \frac{\|\boldsymbol{p}_i - \boldsymbol{p}_M\|^2 - \Delta \bar{z}_i^2[k]}{2\big(\Delta \bar{z}_i[k] + \|\boldsymbol{p}_i - \boldsymbol{p}_M\| \cos(\theta_M[k] - \varphi_i)\big)}. \tag{14}$$

Since $r_j[k] \leq d_M[k]$ and $r_j[k]$ decreases monotonically with respect to $\Delta \bar{z}_i$, it follows that $\Delta \bar{z}_i[k] \geq \Delta d_i[k]$. Thus, we can define $\Delta \bar{z}_i[k] = \Delta d_i[k] + \bar{b}_i[k]$, where $\bar{b}_i[k] \geq 0$. Also, since $r_i[k] \leq r_j[k]$, then by comparing (11) and (14) it follows that $\Delta z_i[k] \geq \Delta \bar{z}_i[k]$, and hence $b_i[k] \geq \bar{b}_i[k]$. Although $\bar{b}_i[k]$ is unknown, the positive term $b_i[k] - \bar{b}_i[k]$, which can be used as a lower bound on $b_i[k]$, is known through $b_i[k] - \bar{b}_i[k] = \Delta z_i[k] - \Delta \bar{z}_i[k]$. Therefore, the lower bound on $b_i[k]$ is obtained as

$$b_i[k] \geq l_i[k] = \Delta z_i[k] - \Delta \bar{z}_i[k]. \tag{15}$$

For the upper bound, we assume that the target position is constrained to be in a closed area with arbitrary shape, where the coordinates of the border are known. In general it is not easy to handle complicated physical constraint on the position in terms of computation. Therefore, we use the geometrical constraints on the position to impose simple bound constraints on the NLOS bias. Let us assume $\boldsymbol{m}[k]$ is the intersection of the AOA line segment and the border of the closed area. Similar to the analysis leading to the lower bound, define

$$\Delta \tilde{z}_i[k] = \|\boldsymbol{m}[k] - \boldsymbol{p}_i\| - \|\boldsymbol{m}[k] - \boldsymbol{p}_M\|. \tag{16}$$

According to (16), $\boldsymbol{m}[k]$ is located on a set of hyperbolas, denoted as $\tilde{H}^b_{iM}$ and representing the points for which the distance difference from the i-th and M-th anchors is $\Delta \tilde{z}_i[k]$. The distance of $\boldsymbol{m}[k]$ from the reference anchor, i.e., $\tilde{r}[k] = \|\boldsymbol{m}[k] - \boldsymbol{p}_M\|$, satisfies

$$\tilde{r}[k] = \frac{\|\boldsymbol{p}_i - \boldsymbol{p}_M\|^2 - \Delta \tilde{z}_i^2[k]}{2\big(\Delta \tilde{z}_i[k] + \|\boldsymbol{p}_i - \boldsymbol{p}_M\| \cos(\theta_M[k] - \varphi_i)\big)}. \tag{17}$$

Since $\tilde{r}[k] \geq d_M[k]$ and $\tilde{r}[k]$ decreases monotonically with respect to $\Delta \tilde{z}_i[k]$, then through a similar argument as used for (12), it follows that $\Delta \tilde{z}_i[k] \leq \Delta d_i[k]$. Also from (16) and the triangle inequality it follows that

$$\Delta d_i[k] \geq \Delta \tilde{z}_i[k] \geq -\|\boldsymbol{p}_i - \boldsymbol{p}_M\|. \tag{18}$$

Therefore, $\Delta \tilde{z}_i[k]$ is a tighter lower bound on $\Delta d_i[k]$, thus a better upper bound on $b_i[k]$ is achieved as

$$b_i[k] \leq u_i[k] = \Delta z_i[k] - \Delta \tilde{z}_i[k]. \tag{19}$$

B. Improved Extended Kalman Filter

The underlying concept of the constrained EKF is similar to the conventional EKF except that a constrained optimization problem is solved at every iteration. At time instant $k-1$, let us assume that $\boldsymbol{s}[k-1|k-1]$ and $\boldsymbol{\Sigma}[k-1|k-1]$ are the estimated state and covariance matrix, respectively. Then at time instant k, we can do the prediction as

$$\begin{aligned} \boldsymbol{s}[k|k-1] &= \boldsymbol{A}_a \boldsymbol{s}[k-1|k-1], \\ \boldsymbol{\Sigma}[k|k-1] &= \boldsymbol{A}_a \boldsymbol{\Sigma}[k-1|k-1] \boldsymbol{A}_a^T + \boldsymbol{B}_a \boldsymbol{Q}_a \boldsymbol{B}_a^T, \end{aligned} \tag{20}$$

where $\boldsymbol{Q}_a$ is the covariance matrix of $\boldsymbol{w}_a[k]$. Using the predicted position, i.e., $[x[k|k-1], y[k|k-1]]^T$, an estimate of the distance $d_i[k]$ between the target and each anchor is computed. These estimates, say $\hat{d}_i[k]$ are used to compute the measurement noise variance $\sigma^2_{n_i}[k]$ according to the model in (3) and hence $\boldsymbol{R}[k]$ is computed according to (6).

Next, we would like to make use of the new range difference and angle measurement vector at the k-th time instant, i.e. $\boldsymbol{y}[k]$ to obtain the filtered state $\boldsymbol{s}[k|k]$ and associated covariance matrix $\boldsymbol{\Sigma}[k|k]$. To this end, we employ a linearization technique based on the Taylor series expansion of the nonlinear function $\boldsymbol{h}(\boldsymbol{s}[k])$ in (5) around the predicted state $\boldsymbol{s}[k|k-1]$:

$$\boldsymbol{h}(\boldsymbol{s}[k]) \approx \boldsymbol{h}(\boldsymbol{s}[k|k-1]) + \boldsymbol{H}[k](\boldsymbol{s}[k] - \boldsymbol{s}[k|k-1]), \tag{21}$$

where $\boldsymbol{H}[k] = \frac{\partial \boldsymbol{h}(\boldsymbol{s}[k])}{\partial \boldsymbol{s}[k]} \,|_{\boldsymbol{s}[k]=\boldsymbol{s}[k|k-1]}$ is the Jacobian matrix derived explicitly in [10]. Therefore, based on this first order expansion we define a linearized measurement vector

$$\begin{aligned} \tilde{\boldsymbol{y}}[k] &= \boldsymbol{y}[k] - \boldsymbol{h}(\boldsymbol{s}[k|k-1]) + \boldsymbol{H}[k]\boldsymbol{s}[k|k-1]. \\ &\approx \boldsymbol{H}[k]\boldsymbol{s}[k] + \boldsymbol{n}[k] \end{aligned}$$

If we denote the prediction error in $\boldsymbol{s}[k|k-1]$ by $\tilde{\boldsymbol{w}}[k|k-1] = \boldsymbol{s}[k] - \boldsymbol{s}[k|k-1]$, which can be considered to be zero mean with covariance $\boldsymbol{\Sigma}[k|k-1]$, then we can combine the linearized range and angular measurements and the predicted state as

$$\begin{bmatrix} \tilde{\boldsymbol{y}}[k] \\ \boldsymbol{s}[k|k-1] \end{bmatrix} \approx \begin{bmatrix} \boldsymbol{H}[k] \\ \boldsymbol{I}_{N+4} \end{bmatrix} \boldsymbol{s}[k] + \begin{bmatrix} \boldsymbol{n}[k] \\ \tilde{\boldsymbol{w}}[k|k-1] \end{bmatrix}, \tag{22}$$

 ISBN: 978-1-61208-284-4

where the covariance matrix of the noise vector is

$$\boldsymbol{C}[k] = \begin{bmatrix} \boldsymbol{R}[k] & 0 \\ 0 & \boldsymbol{\Sigma}[k|k-1] \end{bmatrix}.$$

Now we find $\boldsymbol{s}[k|k]$, the filtered estimate of $\boldsymbol{s}[k]$ by solving the bounded least square problem

$$\begin{aligned} &\min_{\boldsymbol{s}[k]} \left\{ \left\| (\boldsymbol{C}[k])^{-\frac{1}{2}} \Big(\begin{bmatrix} \tilde{\boldsymbol{y}}[k] \\ \boldsymbol{s}[k|k-1] \end{bmatrix} - \begin{bmatrix} \boldsymbol{H}[k] \\ \boldsymbol{I}_{N+4} \end{bmatrix} \boldsymbol{s}[k] \Big) \right\|^2 \right\} \\ &\text{s.t.} \quad l_i[k] \leq b_i[k] \leq u_i[k], \quad i = 1, \ldots, N \end{aligned} \tag{23}$$

Note that in ordinary EKF, (23) is minimized without constraints. In contrast to the unconstrained EKF, (23) is a linear least squares problem with additional bound constraints on the entries of the state vector, and can be solved with moderate computational cost. In our work, we use the Matlab routine `lsqlin`. We can use the nonlinear function $h(\boldsymbol{s}[k])$ in (23) instead of the first order Taylor series approximation, however, the computational complexity would be much higher. Moreover, we did not observe significant improvement in the localization accuracy in our simulation experiments.

To update the covariance, we use as an approximation the recursive formula of the ordinary EKF algorithm, that is

$$\boldsymbol{\Sigma}[k|k] = (\boldsymbol{I} - \boldsymbol{G}[k]\boldsymbol{H}[k])\boldsymbol{\Sigma}[k|k-1], \tag{24}$$

where $\boldsymbol{G}[k]$ is the gain of the EKF

$$\boldsymbol{G}[k] = \boldsymbol{\Sigma}[k|k-1]\boldsymbol{H}^T[k](\boldsymbol{R}[k] + \boldsymbol{H}[k]\boldsymbol{\Sigma}[k|k-1]\boldsymbol{H}^T[k])^{-1}.$$

At this stage, both the state and covariance matrix are corrected and the algorithm continues recursively.

C. Initialization and Algorithm Summary

An initial guess of the position and biases can be made using the single snapshot constrained optimization technique in [6], while the initial values of the velocity components are set to zero, thus $\boldsymbol{s}[0|0]$ is obtained. Since relatively decent estimates of the location and biases are achievable using [6], a relatively moderate diagonal error covariance matrix $\boldsymbol{\Sigma}[0|0]$ is considered. The algorithm is summarized below.

Algorithm 1 Proposed EKF with Bound Constraints

1: **Initialization**:
2: Initialize position and biases using [6] and set $\boldsymbol{v}[0|0] = \boldsymbol{0}$
3: Set $\boldsymbol{\Sigma}[0|0] = \alpha \boldsymbol{I}$ where $\alpha > 0$
4: **for** $k = 1, 2, \ldots, K$ **do**
5: Prediction using (20)
6: Estimate $d_i[k]$, compute $\sigma^2_{n_i}$ in (3) and update $\boldsymbol{R}[k]$
7: Find $\boldsymbol{s}[k|k]$ via the constrained minimization in (23)
8: Update the covariance matrix $\boldsymbol{\Sigma}[k|k]$ using (24)
9: **end for**

IV. Simulation Results

We consider $M = 4$ anchors with fixed positions $\boldsymbol{p}_1 = [0, 10]^T$, $\boldsymbol{p}_2 = [10, 10]^T$, $\boldsymbol{p}_3 = [10, 0]^T$, and $\boldsymbol{p}_4 = [0, 0]^T$, where the units are in meters. The initial position of the target is selected randomly within the square region covered by the anchors. The direction of its velocity vector is initialized randomly while its norm (i.e., speed) is set to 0.4m/s. The location of the target changes over time according to the dynamic model in (7) where the accelerations are normally distributed with $\sigma_x = \sigma_y = 10^{-3}$m/s^2. The trajectory is evaluated for $K = 200$ time samples with a step size $\delta t = 0.1$s. The reference anchor, located at $\boldsymbol{p}_4$, is in LOS, while the other anchors are in NLOS. The exact range values are corrupted by an exponentially distributed NLOS bias with a mean value equal to 0.2 of the true target-anchor range [6]. The additive noise $n_i[k]$ is modelled according to (3) with $\sigma_0 = 10^{-4}$, $\beta = 2$ for the LOS anchor, and $\beta = 3$ for the other NLOS anchors. The true angle of the LOS anchor is also disturbed by a normally distributed error with zero-mean and $\sigma_\theta = 1$deg.

We simulate the proposed constrained EKF described in Algorithm I with bounding constraints on the NLOS biases as derived in Section III-A. We considered both sets of constraints, i.e., the loose bound (10) and the new tighter bounds in (15)-(19), and denote the corresponding algorithms as Constrained EKF I and Constrained EKF II, respectively. In our implementation of these algorithms, we use the true values of σ_x, σ_y, σ_0 and set $\sigma_w = 3$m, although the final performance is robust to some amount of mismatch in these parameters. We compare our result with the single snapshot constrained optimization technique in [6] and the EKF in [10]. The PF is not considered herein since the nonlinearity is not severe and the distribution of the noise is Gaussian. In fact, due to lacking a bound on the biases, the PF approach might perform only slightly better than EKF [10]. The method in [6], is implemented in Matlab by means of `fmincon` function with the choice of SQP technique. Again, we consider both sets of constraints (10) and (15)-(19), and denote the corresponding algorithms as Memoryless I and Memoryless II, respectively. The initialization of Constrained EKF I and Constrained EKF II are done using the Memoryless I and Memoryless II, respectively, while EKF is initialized with Memoryless II. For the initialization of the state covariance matrix, we use $\boldsymbol{\Sigma}[0|0] = 10\boldsymbol{I}_7$, which appears to be reasonable for the considered area and the possible error in position components and biases.

To evaluate the comparative performance of the various tracking algorithms under study, we run Monte Carlo (MC) simulations in Matlab for 500 different starting points and trajectories, generated randomly as specified above. The performance is evaluated in terms of the root mean squared error (RMSE) between the true and estimated vectors. The RMSE in the velocity estimate is also investigated.

The RMSE in positioning is plotted in Fig. 2 for the different techniques under study. We generally find that the performance of the EKF in [10] is strongly dependent on the initialization and its convergence is not always guaranteed due to the absence of bounds on the NOLS biases. The constrained optimization technique in [6] can not yield smooth position estimates due to its memoryless nature, although on the average its performance is satisfactory. We emphasize that the performance of this algorithm is notably improved when the tighter bound given in (15) and (19) is used instead of the simpler one in (10). Initially, Constrained EKF I has a higher RMSE compared to the unconstrained EKF, since it is initialized with a less accurate position. However, within a number of iterations, its performance surpasses that of EKF and Memoryless I. Overall, constrained EKF II exhibits the

 ISBN: 978-1-61208-284-4

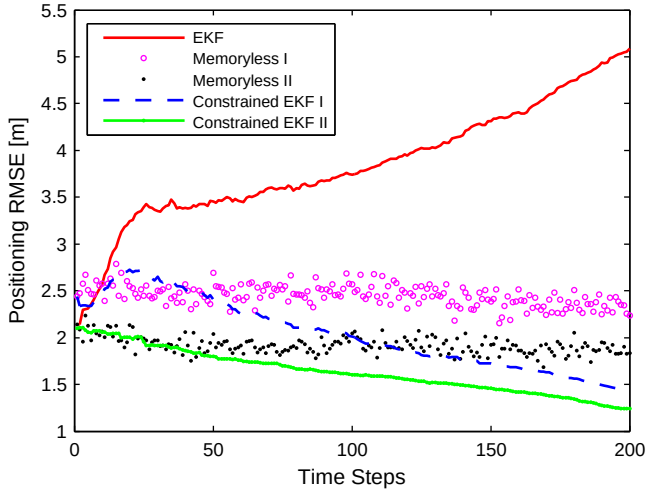

Fig. 2. RMSE of target position vs. time steps.

best performance by a significant margin, which proves the usefulness of our approach.

The RMSE in estimating the velocity components $v_x[k]$ and $v_y[k]$ in Cartesian coordinates is illustrated in Fig. 3. Again, the performance of the newly proposed EKF technique, with bounding constraints on the NLOS biases, exceeds that of EKF by a significant margin.

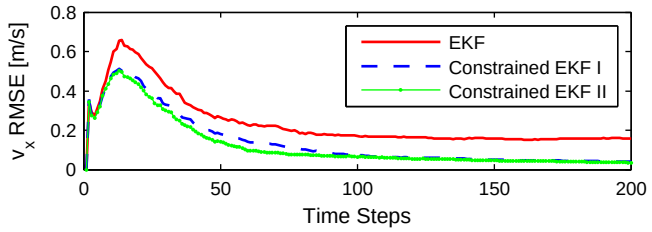

(a) RMSE in estimating v_x

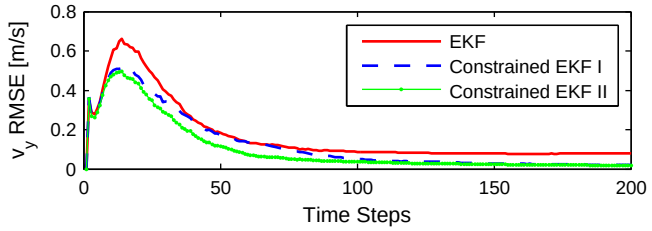

(b) RMSE in estimating v_y

Fig. 3. RMSE of velocity components in logarithm scale vs. time steps.

V. Conclusion

A modified EKF algorithm for localization of a moving target was proposed in this paper, where novel bound constraints on the NLOS bias based on geometrical considerations were incorporated in the filtering (optimization) step of the EKF equations. The main assumption is that at least one LOS anchor remains available for referencing purposes. Through simulations, it was observed that our technique significantly outperformed EKF and memoryless constrained optimization techniques. Our technique shows good robustness against NLOS biases, even when most of the nodes are initially (and remain) under severe NLOS conditions.

Acknowledgment

The authors would like to thank Dr. Kegen Yu of the University of New South Wales in Australia for his helpful comments. This work was supported by a grant from the Natural Science and Engineering Research Council (NSERC) of Canada and by the Fonds québécois de la recherche sur la nature et les technologies (FQRNT).

References

[1] K. Yu, I. Sharp, and Y. J. Gao, *Ground-Based Wireless Positioning*. John Wiley and Sons Ltd., 2009.

[2] S. Gezici, Z. Tian, G. B. Giannakis, H. Kobayashi, A. F. Molisch, H. V. Poor, and Z. Sahinoglu, "Localization via ultra-wideband radios: a look at positioning aspects for future sensor networks," *IEEE Signal Process. Mag.*, vol. 22, pp. 70–84, Jul. 2005.

[3] D. Dardari, R. D'Errico, C. Roblin, A. Sibille, and M. Z. Win, "Ultrawide bandwidth RFID: The next generation?" *Proc. of the IEEE*, vol. 98, no. 9, pp. 1570 –1582, Sep. 2010.

[4] M. Navarro and M. Najar, "Frequency domain joint TOA and DOA estimation in IR-UWB," *IEEE Trans. on Wireless Commun.*, vol. 10, no. 10, pp. 1–11, Oct. 2011.

[5] I. Guvenc and C. C. Chong, "A survey on TOA based wireless localization and NLOS mitigation techniques," *IEEE Communications Surveys Tutorial*, vol. 11, no. 3, pp. 107–124, quarter 2009.

[6] K. Yu and Y. J. Guo, "Improved positioning algorithms for nonline-of-sight environments," *IEEE Trans. on Veh. Tech.*, vol. 57, no. 4, pp. 2342–2353, Jul. 2008.

[7] S. Venkatraman, J. Caffery, and H. R. You, "A novel TOA location algorithm using LOS range estimation for NLOS environments," *IEEE Trans. on Veh. Tech.*, vol. 53, no. 5, pp. 1515–1524, Sep. 2004.

[8] N. J. Thomas, D. G. M. Cruickshank, and D. I. Laurenson, "Performance of a TDOA-AOA hybrid mobile location system," in *Second Int. Conf. on 3G Mobile Communication Technologies*, 2001, pp. 216–220.

[9] C.-D. Wann, Y.-J. Yeh, and C.-S. Hsueh, "Hybrid TDOA/AOA indoor positioning and tracking using extended Kalman filters," in *IEEE Vehicular Technology Conf. Spring*, vol. 3, May 2006, pp. 1058–1062.

[10] M. Najar, J. M. Huerta, J. Vidal, and J. A. Castro, "Mobile location with bias tracking in non-line-of-sight," in *IEEE Int. Conf. on Acoustics, Speech, and Signal Processing*, vol. 3, May 2004, pp. 956–959.

[11] D. B. Jourdan, J. J. Deyst Jr., M. Z. Win, and N. Roy, "Monte carlo localization in dense multipath environments using UWB ranging," in *IEEE Int. Conf. on Ultra-Wideband*, Sep. 2005, pp. 314–319.

[12] J. González, J. L. Blanco, C. Galindo, A. O. d. Galisteo, J. A. Fernández-Madrigal, F. A. Moreno, and J. L. Martínez, "Mobile robot localization based on ultra-wide-band ranging: A particle filter approach," *Robot. Auton. Syst.*, vol. 57, no. 5, pp. 496–507, May 2009.

[13] L. Cong and W. Zhuang, "Nonline-of-sight error mitigation in mobile location," in *Twenty-third Annual Joint Conf. of the IEEE Computer and Communications Societies*, vol. 1, Mar. 2004, pp. 650–659.

[14] S. Maranò, W. M. Gifford, H. Wymeersch, and M. Z. Win, "NLOS identification and mitigation for localization based on UWB experimental data," *IEEE J. Sel. A. Commun.*, vol. 28, no. 7, pp. 1026–1035, Sep. 2010.

[15] S. Venkatesh and R. M. Buehrer, "Non-line-of-sight identification in ultra-wideband systems based on received signal statistics," *Microwaves, Antennas Propagation, IET*, vol. 1, no. 6, pp. 1120–1130, Dec. 2007.

 ISBN: 978-1-61208-284-4